University of Wisconsin Milwaukee
UWM Digital Commons

Theses and Dissertations

December 2021

Construction of Fluorescent Helicase Fusion Proteins for Use in Fret Studies on Helicase Function and Stoichiometry

Moneer Arabiyat
University of Wisconsin-Milwaukee

Follow this and additional works at: https://dc.uwm.edu/etd

 Part of the Chemistry Commons

Recommended Citation

Arabiyat, Moneer, "Construction of Fluorescent Helicase Fusion Proteins for Use in Fret Studies on Helicase Function and Stoichiometry" (2021). *Theses and Dissertations*. 3238.
https://dc.uwm.edu/etd/3238

This Thesis is brought to you for free and open access by UWM Digital Commons. It has been accepted for inclusion in Theses and Dissertations by an authorized administrator of UWM Digital Commons. For more information, please contact scholarlycommunicationteam-group@uwm.edu.

CONSTRUCTION OF FLUORESCENT HELICASE FUSION PROTEINS FOR USE IN FRET STUDIES ON HELICASE FUNCTION AND STOICHIOMETRY

by

Moneer Arabiyat

A Thesis Submitted in

Partial Fulfilment of the

Requirements for the Degree of

Master of Science

in Chemistry

at

The University of Wisconsin-Milwaukee

December 2021

ABSTRACT

CONSTRUCTION OF FLUORESCENT HELICASE FUSION PROTEINS
FOR USE IN FRET STUDIES ON HELICASE FUNCTION AND STOICHIOMETRY

by

Moneer Arabiyat

The University of Wisconsin-Milwaukee, 2021
Under the Supervision of Professor David N. Frick

This thesis details the construction of N-terminal fusions of the *E. coli* helicase DnaB to fluorescent proteins mT-Sapphire and mVenus, and of C-terminal fusions of the hepatitis C virus NS3 helicase (NS3h) to mT-Sapphire and mVenus. These fluorescent fusion proteins were constructed to be used in FRET studies of helicase function and stoichiometry. One example is in assessing the potential oligomerization and cooperativity of NS3h protomers in unwinding RNA. Another potential use is in assessing the stoichiometry of the replisome of *E. coli*; older studies support a dimeric polymerase model of the replisome. Recent studies however suggest that an active replisome which accommodates three polymerase III cores (the trimeric polymerase complex) may be the active form *in vivo* and that the previous dimeric polymerase model may have been incorrect. While most evidence supports the dimeric polymerase complex, there are unanswered questions and FRET could potentially answer these questions.

TABLE OF CONTENTS

List of Figures v

List of Abbreviations vi

Acknowledgements vii

1. Introduction and Background 1
   - Helicases 1
     - Overview 1
     - Ring helicases 1
     - Non-ring helicases 2
   - FRET 2

2. Methods 6
   - DnaB Fusion Proteins 6
     - PCR 6
     - Restriction digests 7
     - Ligations and transformations 7
     - Miniprep and plasmid verification 7
     - Protein expression and purification 8
   - NS3h Fusion Proteins 9
     - PCR/amplicon preparation 9
     - Restriction digests 10
     - Ligations 11
     - Transformations 11
     - Protein expression and purification 13
     - SDS-PAGE 14
     - ATP hydrolysis assays 14

3. Results and Discussion 16

DnaB N-terminus fusions 16
NS3h C-terminus fusions 18
E. coli replisome 19

4. Concluding Remarks 24
5. Figures 25
6. References 36

LIST OF FIGURES

Figure 1: Agarose gel and plasmid map of mVenus-dnaB-pBad plasmid 26

Figure 2: Agarose gel and plasmid map of mT-Sapphire-dnaB-pBad plasmid 27

Figure 3: SDS-PAGE of mVenus-DnaB purification 28

Figure 4: SDS-PAGE of induced mT-Sapphire-dnaB-pBad compared to mVenus-dnaB-pBad..... 29

Figure 5: Agarose gel and plasmid map of mT-Sapphire-dnaB-pet33 plasmid 30

Figure 6: SDS-PAGE of mT-Sapphire-DnaB purification 31

Figure 7: Agarose gel of uncut and cut NS3h fusion plasmids..... 32

Figure 8: SDS-PAGE of VHL purification 33

Figure 9: SDS-PAGE of SHL purification. 34

Figure 10: ATP hydrolysis assay of NS3h fusion proteins compared to wild-type NS3h..... 35

LIST OF ABBREVIATIONS

dH_2O	Distilled water
DEAE	Diethylaminoethanol
FRET	Förster resonance energy transfer
GF	Gel filtration
HCV	Hepatitis C virus
LB	Lysogeny broth
NS3h	Nonstructural protein 3 helicase
SDS-PAGE	Sodium dodecyl sulfate polyacrylamide gel electrophoresis
TAE	Tris-acetate-EDTA

ACKNOWLEDGEMENTS

I'd like to thank my family for their support, and the faculty and colleagues in the lab for their expertise and guidance. It has been a thoroughly enriching experience and I am grateful for the opportunity to expand my knowledge.

1. Introduction and Background

Helicases

Overview

Helicases are proteins which unwind duplex oligonucleotides (i.e., double-stranded DNA, double-stranded RNA, DNA:RNA duplexes, and/or self-annealed RNA), separating the duplex into single strands. They fuel this reaction by hydrolyzing NTPs (typically ATP), utilizing the energy from NTP hydrolysis to translocate along the DNA or RNA and disrupting the hydrogen bonds between complementary base pairs. Helicases play important roles in DNA replication, repair, transcription, and recombination, as well as in RNA processing (Eisen & Lucchesi, 1998).

Helicases can be grouped into one of five superfamilies (SF) based on certain motifs and amino acid sequences (Singleton *et al*., 2007). They can also be classified by translocation direction (5' to 3' or 3' to 5'), and by whether they function as monomers (non-ring types) or as hexamers (the ring type helicases).

Ring helicases

Ring helicases form homohexameric rings which bind ssDNA in their central channel, and the complementary strand passes outside of the ring (Caruthers & McKay, 2002). Each monomer possesses a RecA-like domain for binding and hydrolyzing NTPs. NTPs bind in the cleft between adjacent monomers, for a total of six potential NTP binding sites. Generally speaking, NTP binding, hydrolysis, and release of NDP result in rotation of adjacent subunits, and this rotation underlies the ring-forming helicases ability to translocate along DNA. The exact

mechanism by which the chemical energy of NTP hydrolysis is converted into the mechanical motion of the helicase along DNA, and the nature/order of NTP binding site has yet to be definitively determined and likely varies between different classes of ring-forming helicases. Examples of ring-forming helicases include *E. coli* DnaB and bacteriophage T7 gene product 4 (Lohman & Bjornson, 1996).

Non-ring helicases

In contrast, non-ring helicases function as monomers or possibly dimers. One example of a non-ring helicase is the hepatitis C virus NS3 helicase (NS3h). In the inchworm model, ATP binding and hydrolysis between two RecA-like domains result in a conformational change between the two domains, and this movement results in translocation of the helicase along RNA. An alternative model is the rolling model, in which NS3h is envisioned to function as a dimer (Frick, 2007).

FRET

FRET (fluorescence resonance energy transfer) is the phenomenon by which a donor fluorophore in its excited state de-excites by non-radiatively transferring energy to an acceptor chromophore, which is often but not necessarily also a fluorophore. This non-radiative energy transfer takes place through long-range dipole-dipole coupling. For FRET to take place, donor and acceptor must be selected with appropriate spectral characteristics, i.e., the acceptor chromophore should have a peak excitation frequency that closely matches/overlaps the emission frequency of the donor. FRET is also highly dependent on the distance between donor and acceptor, with the efficiency of energy transfer being inversely proportional to the sixth

power of the distance between them. In general, the distance between donor and acceptor should be between 10 to 75 Å (Selvin 1995). Because of FRET's high dependence on distance, it can be a useful technique for probing protein-protein or other macromolecular interactions as well as distance between them by labeling each with donor and acceptor fluorophores respectively.

In addition to FRET's usefulness in determining relative distances between donor and acceptor, it can also be used to determine stoichiometries of macromolecular (e.g., protein-protein) complexes. Donor fluorescence quenching due to FRET and acceptor emission enhancement due to FRET are related but not necessarily equal quantities, as they depend on the ratio of donors to acceptors in the complex. In one study, FRET was used to determine the stoichiometry of calmodulin (CaM) binding to the calcium channel $Ca_V1.2$ and to the sodium channel $Na_V1.4$, under both basal and elevated Ca^{2+} concentrations in live cells (Ben-Johny *et al.,* 2016). Briefly, plasmids encoding ECFP-tagged CaM (which will function as the donor in the FRET pair) and EYFP-tagged (acceptor in the FRET pair) $Ca_V1.2$ or $Na_V1.4$ were transfected into HEK293 cells. By determining FRET efficiency from both an acceptor-centric metric (i.e., the enhancement of acceptor fluorescence due to FRET) and a donor-centric method (i.e., quenching of donor fluorescence due to FRET), the stoichiometry was determined by dividing $E_{A,\,max}$ (the acceptor-centric FRET efficiency) by $E_{D,\,max}$ (the donor-centric FRET efficiency) which gives the ratio of n_D/n_A (the ratio of donor molecules to acceptor molecules).

In their paper, Ben-Johny *et al*. use the 3^3-FRET and E-FRET methods to resolve the acceptor-centric FRET efficiency and donor-centric FRET efficiency respectively. Both methods make use of three filter cubes: the CFP (ex: ~440 nm, em: ~480 nm), YFP (ex: ~500 nm, em:

~535 nm), and FRET (ex: 440 nm, em: ~535 nm) filter cubes, used to determine a sensitized emission spectrum by way of subtracting corrupting factors (e.g., direct excitation of the acceptor by the initial excitation field, fluorescence emission by donor, etc.). As proof of concept, the authors first construct concatemers of ECFP and EYFP of known stoichiometries and show that the calculated n_D/n_A ratios are accurate. In the experiment with CaM and the ion channels, they show that CaM binds to the Na^+ channel with a 1:1 stoichiometry, and that CaM binds to the Ca^{2+} channel in a 1:1 ratio at basal Ca^{2+} concentrations but binds in a 2:1 ratio at high Ca^{2+} concentration.

In this thesis, fluorescent fusion proteins of two helicases were constructed for use in FRET studies of helicase functions and stoichiometry: fusion proteins of DnaB, the homohexameric ring helicase of the *E. coli* replisome, and of the non-ring HCV NS3 helicase. Fluorescent proteins used were mT-Sapphire and mVenus. The mT-Sapphire protein has an excitation wavelength at 399 nm and an emission wavelength at 511 nm (Ai *et al*., 2008), and the mVenus protein has an excitation wavelength at 515 nm and an emission wavelength at 527 nm (Kremers *et al*., 2006), forming a good FRET paper: mT-Sapphire functioning as donor, and mVenus as acceptor.

DnaB fusions were constructed with fluorescent proteins attached to the N-terminus of DnaB. This was accomplished by cloning the *dnaB* gene from *E. coli* and ligating into pBad vectors which contained genes for mT-sapphire or mVenus. Interestingly, these fusion proteins were active in an ATP hydrolysis assay, but their activity was not stimulated/enhanced by the addition of ssDNA or poly(U) (data not shown), indicating that the presence of the fluorescent protein at the N-terminus may have interfered with their normal function (Reha-Krantz &

Hurwitz 1978). In addition, the N-terminal domain of DnaB has been reported to be important in mediating the helicase activity of DnaB (Biswas *et al.*, 1994).

Four plasmids encoding a fluorescent protein (mT-Sapphire or mVenus) linked to the C-terminus of hepatitis C virus (HCV) NS3 helicase (NS3h) were also constructed. Fluorescent protein gene sequences were cloned from mVenus_pBad and mT-Sapphire_pBad plasmids and ligated into pet24 plasmids encoding NS3h. These include p24-NS3h-mVenus-HL, p24-NS3h-mT-Sapphire-HL, p24-NS3h-mVenus-EL, and p24-NS3h-mT-Sapphire-HL. All four encode a protein that includes, from N-terminus to C-terminus, NS3h-linker region-fluorescent protein-6x His tag. The HL and EL in the names are shorthand for HindIII-linker and EcoRI-linker respectively, in reference to the restriction sites implemented in the two different forward primers used to construct the plasmids resulting in slightly different linker regions. The HindIII-linker between NS3h and the fluorescent protein consists of the amino acid sequence PNSSSVDKL, and the EcoRI-linker has the sequence PNSGSGS.

The abbreviations VHL-p24, SHL-p24, VEL-p24, and SEL-p24 shall herein be used to refer to the plasmids p24-NS3h-mVenus-HL, p24-NS3h-mT-Sapphire-HL, p24-NS3h-mVenus-EL, and p24-NS3h-mT-Sapphire-HL respectively. In addition, the proteins encoded by each of these plasmids shall herein be referred to as VHL, SHL, VEL, and SEL respectively. C-terminal fusion proteins of NS3h were found to be active in an ATP hydrolysis assay and may be useful in identifying potential interactions between NS3h protomers in unwinding assays, as in the rolling model.

2. Methods

DnaB Fusion Proteins:

PCR

Primers were purchased from Integrated DNA Technologies at 100 µM concentrations in IDTE buffer (10 mM Tris, 0.1 mM EDTA, pH 8.0) and with standard desalting. Primers were diluted in 10 mM Tris, pH 8.0 to 5.0 µM concentrations for use in PCR. Primers include regions homologous to *dnaB* gene and a BsrgI and EcoRI restriction site in the dnaB_For and dnaB_Rev primers respectively. Primers used:

dnaB_For: 5'-CGCGCGTGTACAAGGGCAGCGGCAGCGCAGGAAATAAACCCTTCAACAAACAGC

dnaB_Rev: 5'-GCGCGCGAATTCTTATTCGTCGTCGTACTGCGGCCCCGCATAG

PCR reactions were prepared by transferring a single colony of BL21(de3) strain *E. coli* from LB agar plates to 50 µL reaction mixes which included 25 µL of 2x IBI Taq No Dye MasterMix, 10 µL of each 5.0 µM primer, and 5 µL dH_2O. An Eppendorf Mastercycler Realplex 4 PCR machine was used with the following parameters: initial denaturing temperature of 95°C for 5 min, followed by 30 cycles of 95°C for 30 sec, 57°C for 30 sec, and 72°C for 90 sec. Final extension at 72°C for 5 min, followed by a hold temperature of 4°C. PCR products were run on a 1% agarose gel in TAE buffer at 90V, stained with ethidium bromide, and gel extracted with a Thermo Scientific GeneJET Gel Extraction kit.

Restriction digests

PCR amplicons and vectors (mVenus-pBad and mT-sapphire-pBad) were digested with Thermo Scientific Bsp1407I (BsrGI) and Fermentas EcoRI FastDigest in Thermo Scientific 1x Tango buffer at 37°C for 1 hour, run on 1% agarose gels in TAE buffer, stained with ethidium bromide, and gel extracted with a Thermo Scientific GeneJET Gel Extraction kit.

Ligations and transformation

Digested dnaB insert was ligated with digested vector (mVenus-pBad or mT-sapphire-pBad) in roughly a 3:1, 5:1, or 6:1 molar insert:vector ratio using Promega T4 ligase, incubated on ice overnight.

Ligation mixtures were then transformed to NEB 5-alpha Competent *E. coli* (high efficiency) cells by adding 1 µL of ligation reaction mixture to 25 µL of cells in 14 mL Falcon polypropylene round-bottom tubes on ice. Cells then sat on ice for 30 minutes, heat shocked at 42°C in a water bath for exactly 30 seconds, placed on ice for another 5 minutes, and then charged with 475 µL of room temperature SOC media. Cell mixtures were then incubated at 37°C, 250 RPM for 60 minutes before plating 50 µL and 100 µL aliquots of each on LB-Ampicillin agar plates. Plates were incubated at 37°C overnight.

Miniprep and plasmid verification

Several colonies from each transformed plate were selected, grown in 4 mL LB with 50 µg/ml ampicillin at 37°C, 250 RPM for several hours, and 3 mL of each miniprepped using Omega Bio-tek E.Z.N.A. Plasmid DNA Mini Kit. The remaining 1 mL of each culture were charged with 75 µL DMSO and stored at -80°C. Miniprepped plasmids were verified by restriction digest and sequencing.

Protein expression and purification

Cultures of mVenus-dnaB-pBad and mT-sapphire-dnaB-pBad in NEB 5α were grown in LB with 50 μg/ml ampicillin at 37 °C, 250 RPM until OD_{600} was between 0.3 to 0.5, and then induced at room temperature with L-arabinose at concentrations ranging from 0.025% to 0.2% overnight. mT-sapphire-dnaB-pET33 in BL21(de3) was induced with 1 mM IPTG.

Following overnight induction at room temperature, cells were pelleted in a centrifuge at 3200 x *g*, 4°C for 15 minutes and the supernatant discarded. Pellets were resuspended in 50 mL of IMAC5 buffer (50 mM Tris, 5 mM imidazole, 0.5 mM NaCl, pH 7.8) and lysed by sonication in an ice-water bath. Sonication was performed in cycles of 2 minutes on at a 50% duty cycle followed by 3 minutes off, repeated for four cycles. Sonicated cells were then centrifuged at 18,000 x *g* for 30 minutes at 4°C. The crude extract was purified on 1 mL of Ni-NTA Superflow Agarose resin in a small column by hand, washing with 5 x 1 mL fractions of IMAC5, followed by 5 x 1 mL fractions of IMAC40 (50 mM Tris, 40 mM imidazole, 0.5 mM NaCl, pH 7.8), and finally eluting the protein of interest with 3-5 x 1 mL fractions of IMAC500 (50 mM Tris, 500 mM imidazole, 0.5 mM NaCl, pH 7.8).

Protein fractions were further purified as indicated by gel filtration on a ~200 mL Sephacryl S-300 column at 4°C, using Bio-rad BioLogic LP chromatography system, flow-rate= 0.2 mL/min, fraction size= 3.00 mL, GF buffer (20 mM Tris, 100 mM NaCl, 1 mM EDTA, 0.1 mM DTT, pH 7.6).

mT-sapphire-DnaB was further purified by ion exchange chromatography on ~2 mL of DEAE Sepharose Fast Flow resin by hand: Ni column fractions were first desalted on a small

Sephadex G-25 column, and then run through DEAE resin twice, then washed with GF buffer with increasing NaCl concentrations in a stepwise manner.

NS3h Fusion Proteins:

PCR/Amplicon preparation

Primers were purchased from Integrated DNA Technologies at 100 µM concentrations in IDTE buffer (10 mM Tris, 0.1 mM EDTA, pH 8.0) and with standard desalting. Primers were diluted in 10 mM Tris, pH 8.0 to 1.0 µM concentrations for use in PCR. Primers used:

For_HindIII_primer: 5'-GCGCAAGCTTATGGTGAGCAAGGGCGAGGA

For_EcoRI_primer: 5'-GCGCGAATTCGGGTTCTGGTTCTATGGTGAGCAAGGGCGAGGA

Rev_primer: 5'-GCGCCTCGAGCTTGTACAGCTCGTCCATGC

Four 50 µL PCRs were prepared in 0.2 mL PCR tubes as follows: 25 µL of 2x IBI Taq No Dye MasterMix, 10 µL of 1.0 µM For_HindIII_primer or For_EcoRI_primer, 10 µL of 1.0 uM Rev_primer, 0.5 µL of mVenus_pBAD or mT-Sapphire_pBAD (roughly 2.5 ng of either plasmid), and 4.5 µL of ddH_2O. Two negative controls were also prepared containing water in place of template. A Techne TC-312 PCR machine was used with the following parameters: initial denaturing temperature of 95°C for 2 min, followed by 30 cycles of 95°C for 30 sec, 68°C for 20 sec, and 72°C for 1 min. Final extension at 72°C for 5 min, followed by a hold temperature of 4°C.

PCR reaction mixtures were then cleaned using an Omega Bio-tek E.Z.N.A. Plasmid DNA Mini Kit as follows: to each PCR reaction mixture, 200 µL of HBC buffer was added. Reaction mixtures were then loaded on silica spin columns included in kit, centrifuged at 15,000 x *g* for 1

min, and the flow-through discarded. Each column was then washed twice with 700 µL of wash buffer and centrifuged at 15,000 x *g* for 30 sec. Following the second wash, the columns were centrifuged for an additional 2 min at 15,000 x *g* to ensure all ethanol was removed from the column matrix. Amplicons were eluted by adding 50 µL of 10 mM Tris, pH 8.5 to each column, incubating at room temperature for 1 min, and then centrifuging at 15,000 x *g* for 1 min.

Restriction digests

Two restriction digests of recipient plasmid p24-NS3h were prepared as follows: 35 µL of p24-NS3h (estimated concentration ~50 ng/µL), 5 µL of 10x Fermentas FastDigest buffer, 6 µL of dH_2O, 2 µL of Fermentas FastDigest XhoI, and 2 µL of Fermentas FastDigest HindIII or EcoRI. Reactions were incubated at 37 °C for 30 min. Following incubation, 10 µL of NEB 6x purple gel loading dye was added to each reaction mix and run on a 0.5% agarose gel in TAE buffer at 90V. Gel was stained in ethidium bromide and bands gel purified using the Omega Bio-tek E.Z.N.A. Gel Extraction Kit.

Purified PCR amplicons were digested as follows: 35 µL of purified PCR amplicon, 5 µL of 10X Fermentas FastDigest buffer, 8 µL dH_2O, 1 µL of Fermentas FastDigest XhoI, and 1 µL of Fermentas FastDigest HindIII or EcoRI (PCRs using the For_HindIII_primer were digested with the HindIII restriction enzyme, and those using the For_EcoRI_primer were digested with EcoRI restriction enzyme). Reactions were incubated at 37°C for 30 min. Following incubation, digested amplicon was purified using the Omega Bio-tek E.Z.N.A. Plasmid DNA Mini Kit as described previously.

Restriction digests of the final plasmids were performed to verify correct sequence using HindIII, SmaI/NdeI, and PstI. Restriction digests were run on a 0.7% agarose gel in TAE buffer at 70V and then stained in ethidium bromide.

Ligations

Gel-purified HindIII/XhoI-cut p24-NS3h was ligated with purified HindIII/XhoI-cut amplicons by combining on ice: 6 µL of cut p24-NS3h (~45 ng DNA), 0.8 µL of cut amplicon (~15 ng DNA) or dH_2O (negative control), 1 µL of 10x T4 buffer, 2 µL dH_2O, and 0.2 µL of Promega T4 ligase (0.6 Weiss units). Reaction mixtures sat in ice in foam bucket on room temperature shelf overnight.

Gel purified EcoRI/XhoI-cut p24-NS3h was ligated with purified EcoRI/XhoI-cut amplicons using NEB Instant Sticky-end Ligase as follows: 4.4 µL of cut p24-NS3h (~35 ng) and 0.6 µL of cut amplicons (~12 ng) or dH_2O (negative control) were combined at room temperature (corresponding to about a 3:1 insert:vector molar ratio). Mixtures were then placed on ice, and 5 µL of 2x Instant Sticky-end Ligase Master Mix was added to each, mixed by gently pipetting reaction mixtures up and down several times. Reactions sat on ice for an additional 5 minutes before being transformed.

Transformations

Ligation mixtures were transformed to NEB 5-alpha Competent *E. coli* (high efficiency) cells by adding 1 µL of ligation reaction mixture to 25 µL of cells in 14 mL Falcon polypropylene round-bottom tubes on ice. Cells then sat on ice for 30 minutes, heat shocked at 42°C in a water bath for exactly 30 seconds, placed on ice for another 5 minutes, and then charged with 475 µL of room temperature SOC media. Cell mixtures were then incubated at 37°C, 250 RPM

for 60 minutes before plating 50 µL and 100 µL aliquots of each on LB-Kanamycin agar plates. Plates were incubated at 37°C overnight.

Instant Sticky-end ligase reaction mixture transformations had >50 colonies on the 50 µL-aliquoted plates and >100 colonies on the 100 µL-aliquoted plates. Each negative control plate had 8 colonies. Four colonies were picked from each 100 µL-aliquoted plate and each incubated in 5 mL of LB plus 50 µg/ml kanamycin at 37°C, 250 RPM for 9 hours. Following incubation, 1 mL was removed from each culture and charged with 75 µL DMSO for storage at -80°C. The remaining volumes of each culture were harvested for plasmid DNA using the Omega Bio-tek E.Z.N.A. Plasmid DNA Mini Kit.

Promega T4 ligase reaction mix transformations showed several hundred colonies on each plate, with lawns of cells on some areas of the 100 µL-aliquoted plates. The negative control plates showed 1 colony on the 50 µL-aliquoted plate and 6 colonies on the 100-µL aliquoted plate. Two colonies were picked from each 50 µL-aliquoted plate and each incubated in 5 mL of LB plus 50 µg/ml kanamycin at room temperature, 200 RPM overnight. Following incubation, 1.0 mL was removed from each culture and charged with 75 µL DMSO for long-term storage at -80°C before harvesting the remaining volume of cells for plasmid DNA as described previously.

Following verification of successful C-terminal fluorescent NS3h plasmid constructs by restriction digests, plasmids were transformed to BL21(DE3) Competent *E. coli* cells following the same transformation protocol described previously.

Protein expression and purification

Transformed BL21(DE3) cells were grown in 0.5L of LB + Kanamycin in 2L Erlenmeyer flasks at 37°C, 250 RPM until reaching an OD_{600} between 0.2 and 0.4. Cells were then allowed to cool to room temperature for approximately 30-45 minutes before inducing with 0.5 mM IPTG. Cells were then incubated overnight at room temperature, 200 RPM.

The following day, induced cells were centrifuged at 1,000 x *g* for 60 minutes at 4°C and the supernatant discarded. Cell pellets were stored at -20°C until ready to be lysed.

Induced cell pellets were resuspended in 25 mL of IMAC5 buffer (50 mM Tris, 5 mM imidazole, 0.5 mM NaCl, pH 7.8) and lysed by sonication in an ice-water bath. Sonication was performed in cycles of 2 minutes on at a 50% duty cycle followed by 3 minutes off, repeated for four cycles. Sonicated cells were then centrifuged at 13,000 x *g* for 45 minutes at 4 °C. The crude extract was purified on 1 mL of Ni-NTA Superflow agarose resin in a small column by hand, washing with 5 x 1 mL fractions of IMAC5, followed by 5 x 1 mL fractions of IMAC40 (50 mM Tris, 40 mM imidazole, 0.5 mM NaCl, pH 7.8), and finally eluting the protein of interest with 3-5 x 1 mL fractions of IMAC500 (50 mM Tris, 500 mM imidazole, 0.5 mM NaCl, pH 7.8).

Following elution from the nickel column, the fraction(s) with the highest concentration of protein were further purified by gel-filtration (GF) chromatography on a Sephacryl S-300 column (diameter 1.5 cm, bed volume ~75 mL). For the VHL and SHL proteins, the buffer used was 20 mM Tris, 100 mM NaCl, 1 mM EDTA, 0.1 mM DTT, pH 7.6. In order to improve binding of the protein to DEAE resin in the subsequent and final step of purification, the NaCl concentration of the buffer used for GF chromatography was decreased to 50 mM for the

remaining two proteins (VEL and SEL). GF chromatography was performed at 4°C with a Bio-rad BioLogic LP chromatography system, flow-rate= 0.1 mL/min, fraction size= 1.5 mL.

The final step of purification was performed on DEAE resin. The most concentrated GF fractions were combined and loaded on ~1 mL of DEAE Sepharose Fast Flow resin and eluted by a stepwise increasing concentration of NaCl in GF buffer.

SDS-PAGE

Protein samples were prepared for SDS-PAGE by diluting in dH_2O if necessary, adding 6x SDS-loading dye to a 1x concentration, and heating at 95°C for 10 minutes. Samples were then allowed to cool to room temperature before storing at -20°C until ready to be used. SDS-PAGE was performed using 10% gels. Marker/ladder used was Thermo Scientific Unstained Protein MW Marker (cat. no. 26610). SDS-PAGE was performed at 50V until the samples reached the resolving gel and then increased to 100V for the remainder of the run. Gels were stained in Coomassie Brilliant Blue stain overnight with gentle agitation on a rocking shaker and then de-stained in water for several hours until background was clear.

ATP hydrolysis assays

ATP hydrolysis reactions were carried out at 23 °C in 25 mM MOPS pH 6.5, 2 mM $MgCl_2$, 20 µM poly(U) (average length 2500 nt, concentration is reported in terms of free nucleotide concentration), 20 nM of enzyme, and various concentrations of ATP. Total reaction volumes were 50 µL, and reactions were initiated with the addition of the enzyme. Reactions were terminated after 10 minutes with the addition of 800 µL malachite green reagent (3:1 mix by volume of solutions of 0.045% malachite green and 4.2% ammonium molybdate in 4.0N HCl, and 0.025% Tween 20, prepared within an hour before reactions were carried out), mixed

thoroughly, and then immediately adding 100 µL of a 35% sodium citrate solution. Absorbance at 630 nm of each reaction mix was taken 15 minutes following the addition of the malachite green reagent to allow the color to develop, and absorbance readings were converted to concentration of phosphate (P_i) using a standard curve.

3. Results and Discussion

DnaB N-terminus fusions

Figure 1 and Figure 2 show agarose gels and plasmid maps of mVenus-dnaB-pBad and mT-Sapphire-dnaB-pBad respectively and are consistent with expectations. Genes were also verified by sequencing. In Figure 3, mVenus-DnaB fractions are shown in SDS PAGE and demonstrate the successful purification of the protein by Ni affinity chromatography followed by gel filtration chromatography. Concentrated protein fractions were noticeably bright yellow.

In contrast, mT-Sapphire-DnaB failed to express from the constructed mT-Sapphire-dnaB-pBad plasmid. This was particularly strange, as mT-Sapphire differs from mVenus by only a few residues, and given the good expression of mVenus-DnaB, similar levels of expression would be expected of the mT-Sapphire fusion. The expected gene sequence of the plasmid was verified by sequencing, ruling out the possibility of a nonsense mutation.

Several cultures of mT-Sapphire-dnaB-pBad in NEB5α were induced with varying concentrations of arabinose (ranging from 0.025% to 0.2%, as well as an uninduced control) and whole cell protein run on SDS PAGE. As a positive control to compare against, mVenus-dnaB-pBad in NEB5α were also induced and whole cell protein run (both the mVenus and mT-Sapphire fusions are roughly the same size, 83.3 kDa, and should migrate the same distance). The SDS PAGE is shown in Figure 4 and reveals that at none of the arabinose concentrations used was mT-Sapphire-DnaB expressed; in contrast, mVenus-DnaB is clearly visible. This result rules out the possibility that mT-Sapphire-DnaB was ending up in inclusion bodies.

Curiously, a closer comparison of the sequences of mT-Sapphire-dnaB-pBad and mVenus-dnaB-pBad revealed a small difference in the ribosomal binding site. While the difference seemed unlikely to have any profound effect, it was the only plausible explanation for the failure to express the mT-sapphire fusion. Fortuitously, the entire mT-Sapphire-dnaB gene could be easily cut from the pBad vector (leaving behind the ribosomal binding site) and ligated into pet33 by digestion with NheI and HindIII.

The digestion and ligation of mt-Sapphire-dnaB into pet33 was carried out and the constructed plasmid (mT-Sapphire-dnaB-p33) verified on agarose gel shown in Figure 5 along with a plasmid map. This time, protein was successfully expressed upon inducing with IPTG and SDS PAGE of the purified protein shown in Figure 6. The concentrated protein fractions were visibly green and under UV fluoresced brightly blue. Protein was purified by Ni affinity chromatography, followed by DEAE chromatography.

Purified mVenus-DnaB and mT-Sapphire-DnaB were both active in an ATP hydrolysis assay, but only weakly, and their activity was not stimulated by the addition of ssDNA (data not shown). Unfortunately, this indicates that the fusion of the fluorescent proteins to the N-terminus of DnaB perturbed their normal function. Given these results, a C-terminal fusion of DnaB may be necessary and should be assessed in future studies.

NS3h C-terminus fusions

Following successful transformation of NEB-5α Competent *E. coli* cells with the ligation reaction mixtures, plasmids were harvested, and multiple restriction digests performed to verify that the correct/expected constructs were formed.

In Figure 7, an agarose gel of each of the four constructed plasmids, both uncut and digested with HindIII or SmaI/NdeI display the expected band patterns/sizes, indicating successful construction of the plasmids.

Figures 8 and 9 show SDS-PAGE results of the protein purification. Protein bands appear at the expected size (~80 kDa) following purification. Of note from the SDS-PAGE, the GF chromatography step appears to provide very little if any improvement in purity. In the future, it may be better to replace the GF step with a simple desalting step to prepare the eluted nickel fractions for loading on the DEAE column, saving time, and likely improving yield, with little to no impact on final purity. It is also worth noting that in 100 mM NaCl, the proteins will still bind to the DEAE resin, albeit with slightly reduced efficiency (see DEAE column flow-through in lane 9 of Figure 8 and lane 7 of Figure 9, where some of the protein was still present).

Figure 10 shows the ATP hydrolysis assay of the fusion NS3h proteins compared to WT NS3h. Calculated Vmax [95% CI] for WT NS3h, VHL, SHL, and SEL were 35.1 [30.9, 40.0], 31.1 [27.0, 36.1], 32.3 [28.2, 37.9], and 32.1 [27.7, 37.4] μM/min respectively. Calculated k_{cat} [95% CI] were 1755 [1545, 2000], 1555 [1350, 1805], 1630 [1410, 1895], 1605 [1385, 1870] min^{-1} respectively. Calculated K_M [95% CI] of ATP were 193 [86.7, 340], 181 [65.8, 347], 189 [70.5, 362], and 154 [42.4, 317] μM ATP respectively. In all cases of the fusion proteins, the calculated

Vmax and k_{cat} was slightly lower than that of wild-type NS3h, and may be a result of differences in protein purity, preparation, storage, or simply error in the measurements, etc.; alternatively, the presence of the fluorescent fusion protein may impart a slight negative effect on Vmax. Further experiments would need to be conducted to determine definitively. In any case, the difference is relatively small, and the ATP hydrolysis assay show that fusions of fluorescent proteins to the C-terminus of NS3h retain activity. These C-terminal fusions of NS3h might be useful in FRET studies investigating the dynamics of NS3h translocation on RNA. The plasmids themselves may also serve as useful templates for construction of other C-terminal fluorescent fusion proteins.

E. coli replisome

At the heart of the replisome of *Escherichia coli* is the DNA polymerase III holoenzyme, which contains polymerase III (αεθ), the β-clamp, and the clamp loader complex, also known as the gamma complex. The pol III holoenzyme is responsible for replicating the *E. coli* genome.

The clamp loader complex consists of seven subunits: one unit of χ, one of ψ, one of δ, one of δ', and three subunits derived from the *dnaX* gene. The *dnaX* gene encodes for two possible proteins: a full-length τ-subunit, and a truncated version which results from a programmed translation frameshift, called the γ-subunit, for which the gamma complex was named. Compared to the full-length τ-subunit, the γ-subunit lacks the fourth and fifth domains of τ, which are involved in binding to DnaB (the helicase involved in DNA replication in *E. coli*) and to the α unit of pol III, respectively. Importantly, τ will bind and coordinate a replicative pol III enzyme, whereas γ will not.

The composition of the gamma complex was for a long time believed to contain two τ subunits and one γ subunit ($\tau_2\gamma_1\delta\delta'\chi\psi$), in which case it can bind two pol III enzymes, hence the occasional reference to this composition as the *dimeric polymerase form*. Evidence for this composition included purification and stoichiometric determination of the pol III holoenzyme (Hawker & McHenry, 1987; Pritchard *et al.,* 2000) and that γ occupied a unique spot in the clamp loader complex (Glover & McHenry, 2000).

However, τ can be cleaved by OmpT protease to generate a protein roughly the same size as γ, being only two residues shorter than authentic γ (Dallman *et al.*, 2000). This, coupled with the open question on why the clamp loader complex should include a truncated version of DnaX which possesses fewer domains (and, therefore, presumably less functionality), raised doubts about whether γ was truly present in the clamp loader complex, or if the apparent presence of γ was actually an artifact of OmpT proteolysis of τ.

A trimeric polymerase form of the pol III holoenzyme could be constructed *in vitro*, whereby the clamp loader complex consisted of three τ subunits and no γ ($\tau_3\delta\delta'\chi\psi$), and this trimeric polymerase form was shown to be fully functional in DNA replication (McInerney *et al.*, 2007). The authors proposed that two of the three pol III enzymes may function on the lagging strand. It is important to note that the trimeric polymerase form was assembled *in vitro* by mixing the individual components of the holoenzyme together, without including the γ-subunit. That said, this study demonstrated that the trimeric polymerase form could indeed be formed and that it is functional, at least *in vitro*.

A paper supporting the trimeric polymerase form *in vivo* utilized slimfield fluorescence microscopy to show that there were three units of τ per active replisome, and consistent with the presence of three τ subunits, three subunits each of α and ε, which comprise part of the pol III core (Reyes-Lamothe *et al.,* 2010). In this paper, YPet fusion derivatives of chromosomally encoded replisome proteins were expressed in live cells and a compact Gaussian laser excitation field used to excite single cells, and the resulting fluorescence measured every 3 ms over 90 ms. By comparing the resulting fluorescence spectra obtained to single YPet molecules immobilized and excited in the same manner *in vitro*, the authors were able to determine the number of each replisome component present in the replisome. Consistent with the literature (McHenry *et al.,* 2011), the number of subunits of DnaB, a hexameric helicase, and of δ, were determined to be 6 and 1 respectively, lending a degree of credibility and soundness to the technique.

However, interestingly, one of the results from the slimfield microscopy paper appears inconsistent with the trimeric polymerase model; or, at the very least, leaves some doubt on the accuracy of the reported stoichiometries. One of the strains used was the *dnaX* γ^- mutant, in which the original frameshifting sequence of *dnaX* was mutated to prevent the frameshift (gcaaaaaagagtga mutated to gcGaaGaagagtga), so that this strain only produces τ and not γ (Blinkova *et al.,* 1993). The *dnaX-YPet* fusion of this γ-less strain indicated a total of not three, but four τ subunits in the replisome. This is inconsistent with the literature which widely agrees that there are only three total subunits of DnaX in the clamp loader complex, and is inconsistent with the paper itself; if the clamp loader complex truly contains three τ subunits and no γ subunits as stated in the preceding paragraph, why should the γ-less *dnaX* mutant

strain have any effect on the reported stoichiometry of the clamp loader complex? The stoichiometry with the γ-less strain would be expected to be the same as in the normal *dnaX* strain. One of the possibilities for this apparent discrepancy is an error in the calibration curve. Another possibility is the presence of more than one clamp loader complex and/or individual components of the pol III holoenzyme in some replication forks. Herein lies one of the problems with the technique. Even with perfect calibration, it only determines the total number of a particular subunit/peptide in an area. It makes no distinction between those subunits that are part of a complex, and those that are not, nor does it distinguish the possibility of multiple complexes being present.

Finally, it was reported recently that contrary to the aforementioned study, the active replisome *does* contain γ and is a dimeric polymerase (Dohrmann *et al.,* 2016). In this study, the γ-less *dnaX* mutant strain was used and transformed with a plasmid encoding γ with a C-terminal biotin tag. In this system, γ could only be expressed from the plasmid, and would contain a C-terminal biotin tag. Purification of the pol III holoenzyme and analysis by SDS-PAGE revealed that γ was present and probing with streptavidin showed that it contained the biotin tag. This experiment demonstrated unequivocally that γ is part of the pol III holoenzyme, and not merely an artifact of proteolysis of τ, because if the latter were the case, the biotin tag would not have been present. In conjunction with the previous studies that identify γ as a member of the pol III holoenzyme, the evidence convincingly indicates that *in vivo* the pol III holoenzyme is a dimeric polymerase and that it does contain γ.

However, there remains some unanswered questions. The γ-less *dnaX* mutant strain presumably *does* exhibit the trimeric polymerase form (i.e., with the clamp loader complex

existing with $\tau_3\delta\delta'\chi\psi$ stoichiometry, as it is incapable of producing γ) and is apparently viable, albeit with increased sensitivity to UV radiation and reduced mutagenic break repair (Dohrmann *et al.,* 2016). Given that the trimeric polymerase form is both possible and functional in DNA replication, it's interesting to wonder if under certain circumstances *E. coli* might employ the trimeric form in DNA replication.

FRET may be useful in studying the stoichiometry of the replisome *in vivo*. For example, τ could be labeled with a donor, and another protein that it associates with (such as DnaB) could be labeled with acceptor, or vice versa. The dimeric (two τ subunits) vs the trimeric (three τ subunits) would therefore give different ratios of $E_{A,\,max}$: $E_{D,\,max}$, and it could be determined with more confidence which stoichiometry is relevant *in vivo*, or if there are factors that cause the stoichiometry to switch from one form to another.

4. Concluding Remarks

Several plasmids encoding fluorescent fusion proteins of helicases DnaB and HCV NS3h were successfully created and may prove useful in studies of these proteins. mT-Sapphire and mVenus form a good FRET pair, and FRET can be a useful technique to probe stoichiometries or interactions *in vivo* that may be otherwise difficult to measure, particularly if the interaction is transitory in nature and/or highly dependent on specific circumstances within the cell. For example, such FRET experiments may be useful in studying the stoichiometry of the replisome components in *E. coli*, where some controversy still exists on whether the dimeric or the trimeric polymerase model is the active form *in vivo*. FRET can also be used to probe the mechanisms of these helicases, including assessing the rolling mechanism that has been proposed for HCV NS3h, in which two protomers function together as a dimer to unwind duplex RNA; such an interaction could be detectable by FRET.

5. Figures

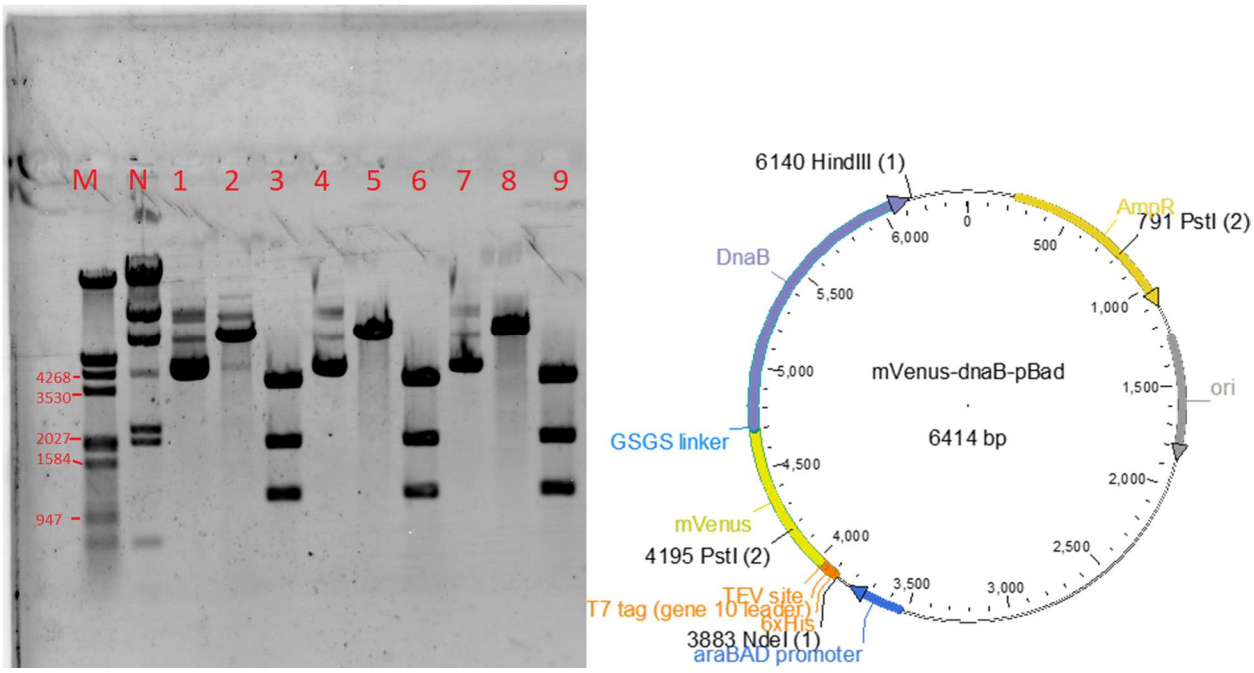

Figure 1: **Agarose gel and plasmid map of mVenus-dnaB-pBad plasmid.** M: Lambda DNA/EcoRI+HindIII marker. N: Lambda DNA/HindIII marker. Lanes 1, 4, and 7: Uncut mVenus-dnaB-pBad plasmid from three separate colonies following transformation. Lanes 2, 5, and 8 are NdeI digests of plasmids in lanes 1, 4, and 7 respectively. Expected to cut once producing a band of size 6414 bp. Lanes 3, 6, and 9 are HindIII+PstI digests of plasmids in lanes 1, 4, and 7 respectively. Expected band sizes of 3404, 1945, and 1065 bp. Plasmid map with restriction sites used is shown.

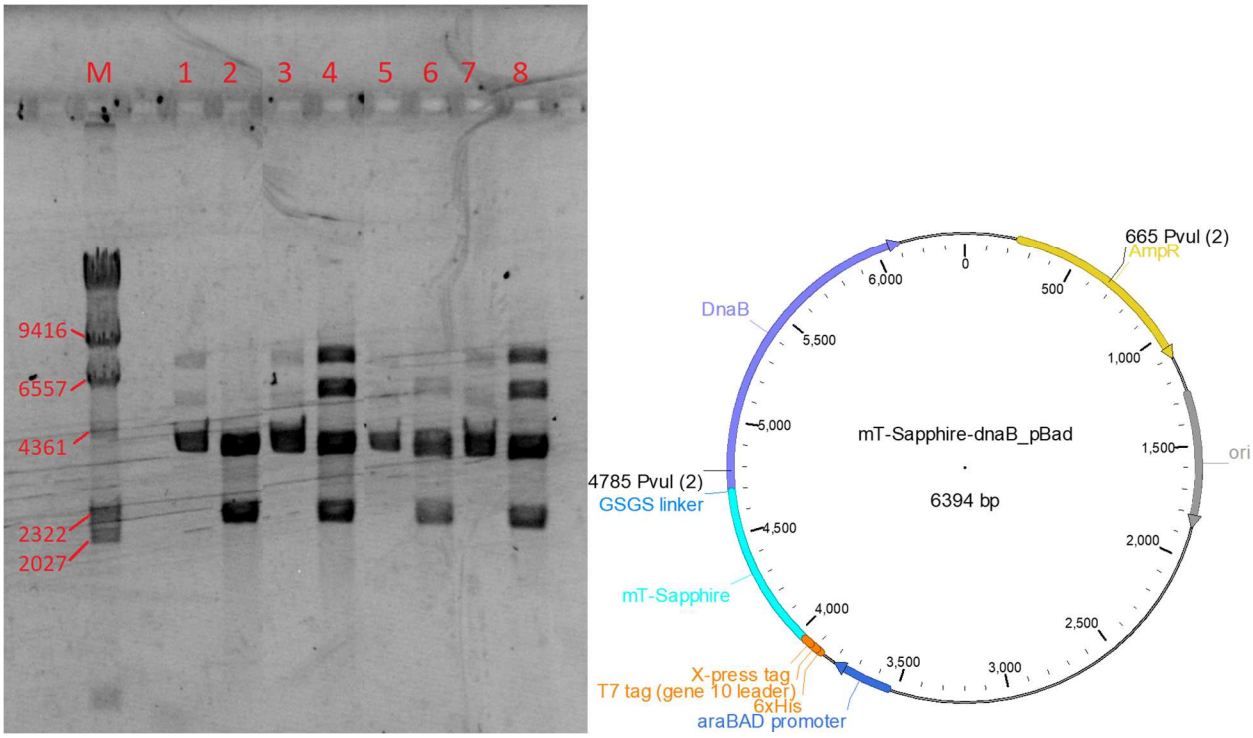

Figure 2: **Agarose gel and plasmid map of mT-Sapphire-dnaB-pBad plasmid.** M: Lambda DNA/HindIII marker. Lanes 1, 3, 5, and 7: Uncut mT-Sapphire-dnaB-pBad plasmid from four separate colonies following transformation. Lanes 2, 4, 6, and 8 are PvuI digests of plasmids in lanes 1, 3, 5, and 7 respectively. Expected to cut twice producing bands of 4120 and 2274 bp. Lanes 2 and 6 as expected. Lanes 4 and 8 have two additional clearly visible bands; one at ~6400 bp can be attributed to plasmid that was only cut once. The other band eluting at ~9400 bp is of unknown origin, therefore only colonies cognate to lanes 1 and 5 were used for subsequent work. Plasmid map with restriction sites used is shown.

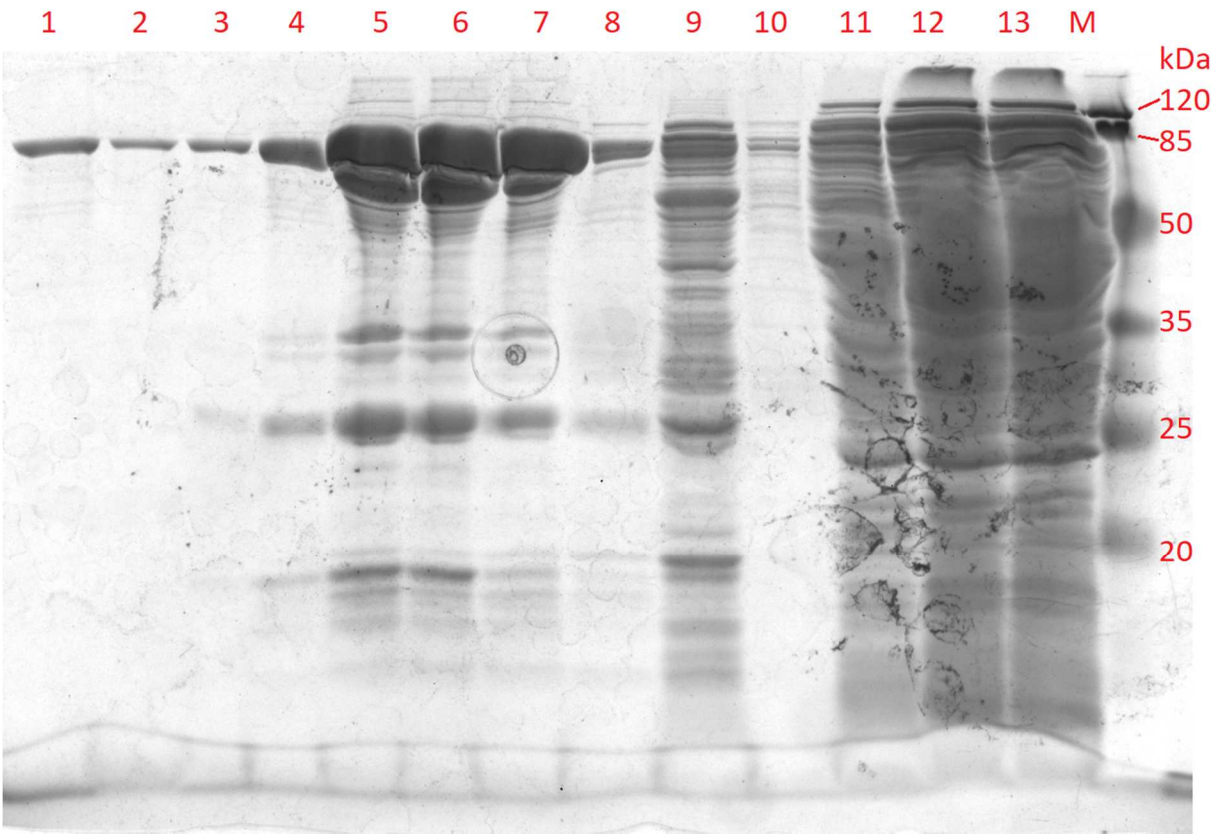

Figure 3: **SDS-PAGE of mVenus-DnaB purification**. Lanes 1 and 2: Protein fractions 36 and 34 respectively off gel filtration column. Lanes 3-7: Fractions eluted off Ni column with +500 mM imidazole, fractions #1-5 respectively. Lanes 8 and 9: Fractions eluted off Ni column with +40 mM imidazole, fractions #5 and #1 respectively. Lanes 10 and 11: Fractions eluted off Ni column with +5 mM imidazole, fractions #5 and #1 respectively. Lane 12: Flow-through off Ni column. Lane 13: Crude extract. M: Thermo MW Markers cat. no. 26612.

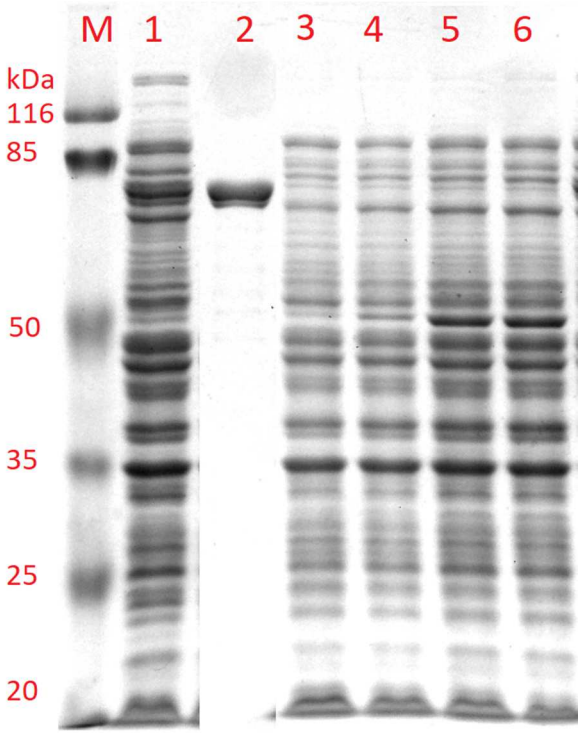

Figure 4: **SDS-PAGE of induced mT-Sapphire-dnaB-pBad compared to mVenus-dnaB-pBad.** M: Thermo MW Markers cat. no. 26612. Lane 1: Whole cell proteins of induced mVenus-dnaB-pBad in NEB 5α cells (used as positive control; mVenus-dnaB visible at ~83.3 kDa). Lane 2: Purified mVenus-dnaB. Lanes 3-6: Whole cell proteins of induced mT-Sapphire-dnaB-pBad in NEB 5α cells, arabinose concentrations 0.2%, 0.1%, 0.05%, and 0.025% respectively. Samples prepared 15 hours after induction at room temperature. mT-Sapphire-dnaB clearly not visible, ruling out the possibility that the protein was ending up in inclusion bodies.

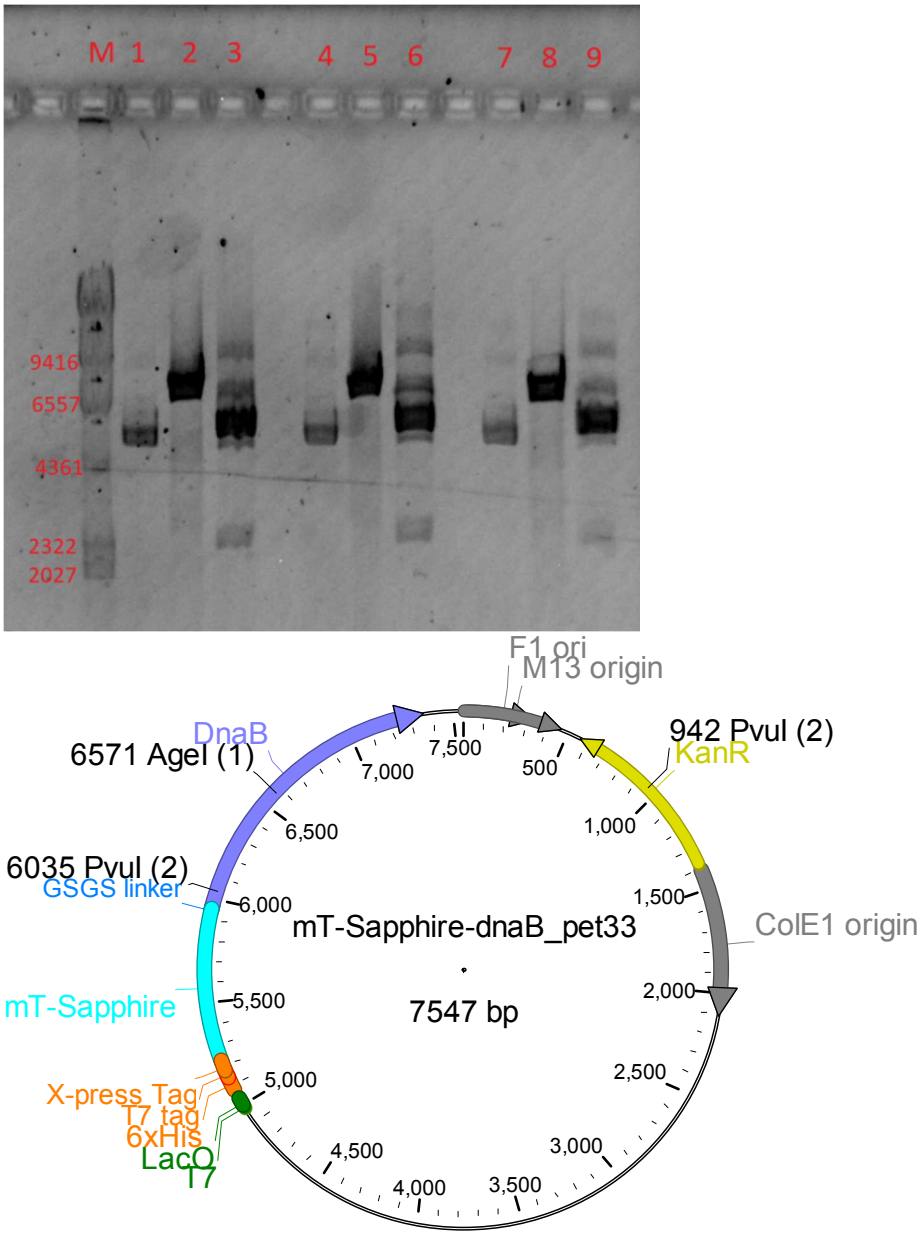

Figure 5: **Agarose gel and plasmid map of mT-Sapphire-dnaB-pet33 plasmid**. M: Lambda DNA/HindIII marker. Lanes 1, 4, and 7: Uncut plasmid from three separate colonies after transformation. Lanes 2, 5, and 7: AgeI digest of plasmid in lanes 1, 4, and 7 respectively. With AgeI, single cut expected producing a band at 7547 bp. Lanes 3, 6, and 9: PvuI digest of plasmid from lanes 1, 4, and 7 respectively. With PvuI, expected to see cut twice producing two bands at 5093 and 2454 bp. Both bands are present, as well as the “cut once” band at 7547 bp. All lanes consistent with expected plasmid. Plasmid map with restriction sites used is shown.

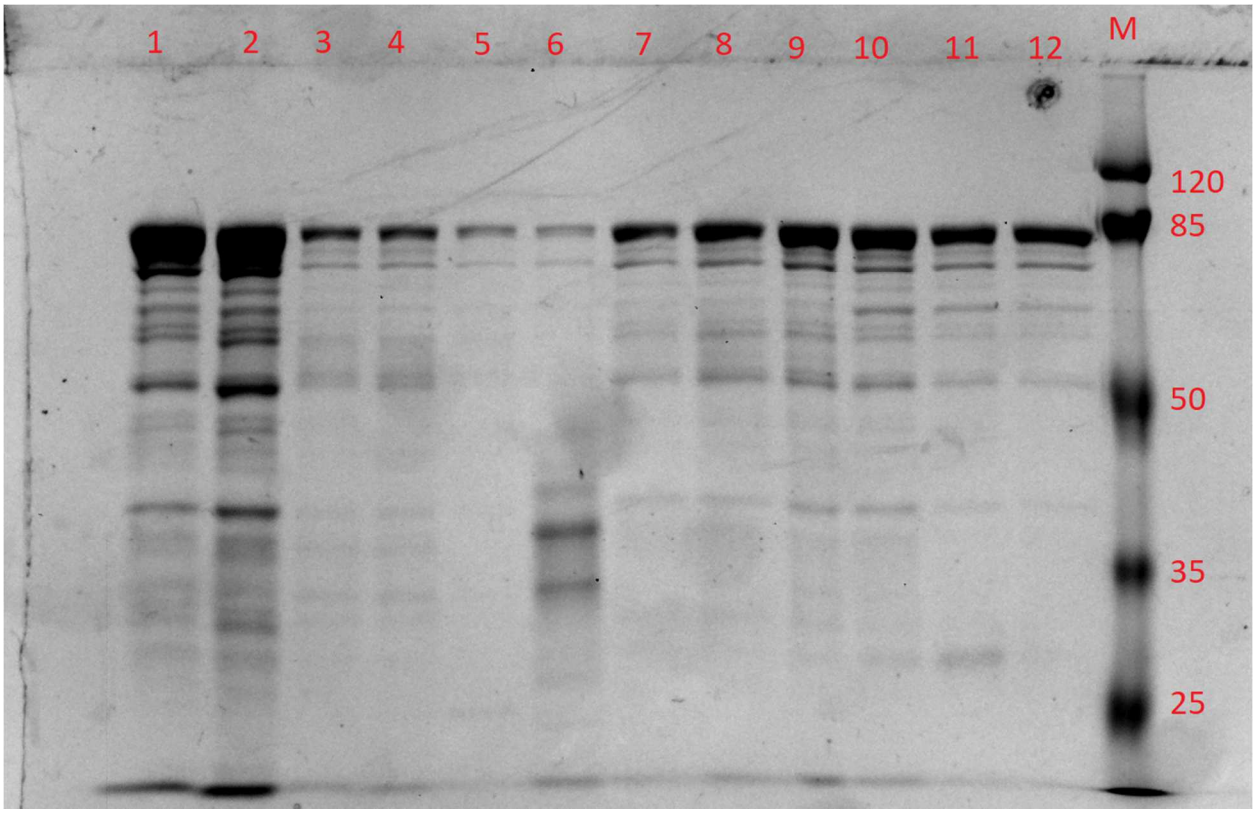

Figure 6: **SDS-PAGE of mT-Sapphire-DnaB purification.** M: Thermo MW Markers cat. no. 26610. Lane 1: Fraction eluted off Ni column with +500 mM imidazole. Lane 2: Desalted protein fraction following Ni column isolation. Lane 3: Flow-through after loading desalted fraction on DEAE column. Lane 4 and 5: Washes 1 and 2 with GF buffer on DEAE column. Lane 6: Elution with +100 mM NaCl. Lane 7-9: Elution fractions with +200 mM NaCl. Lanes 10-12: Elution fraction with +400 mM NaCl.

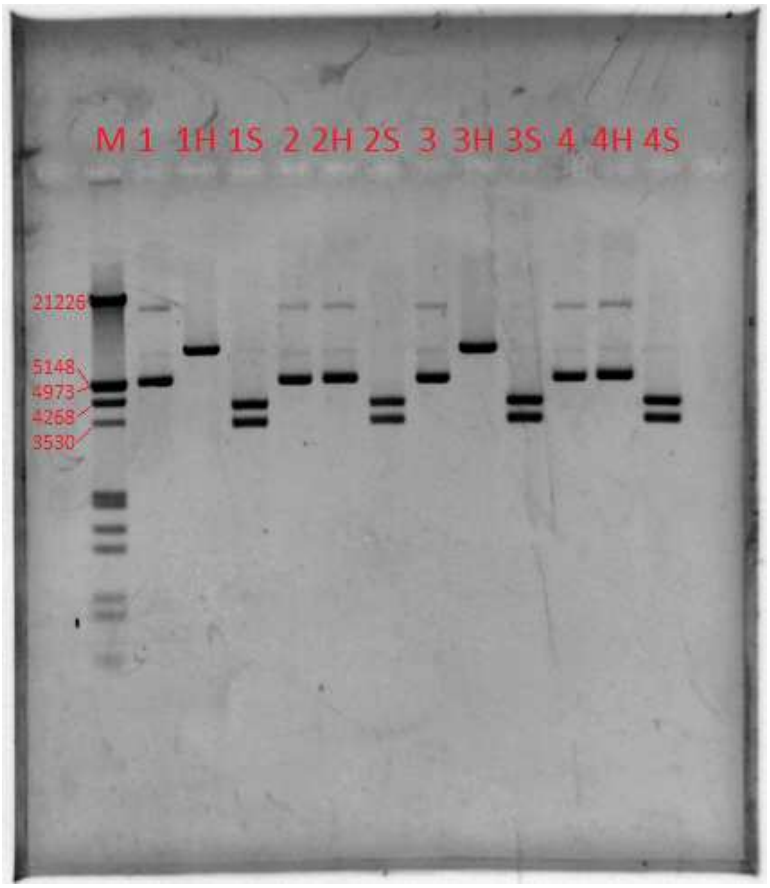

Figure 7: **Agarose gel of uncut and cut NS3h fusion plasmids.** M: 200 ng of λ-HindIII/EcoRI marker, 1: uncut VHL-p24, 1H: VHL-p24 with HindIII (expected band 7406 bp), 1S: VHL-p24 with SmaI/NdeI (expected bands 4002 and 3404 bp), 2: uncut SHL-p24, 2H: SHL-p24 with HindIII (expected uncut), 2S: SHL-p24 with SmaI/NdeI (expected bands 4002 and 3404 bp), 3: uncut VEL-p24, 3H: VEL-p24 with HindIII (expected band 7400 bp), 3S: VEL-p24 with SmaI/NdeI (expected bands 4002 and 3398 bp), 4: uncut SEL-p24, 4H: SEL-p24 with HindIII (expected uncut), 4S: SEL-p24 with SmaI/NdeI (expected bands 4002 and 3398 bp). All lanes ran as expected.

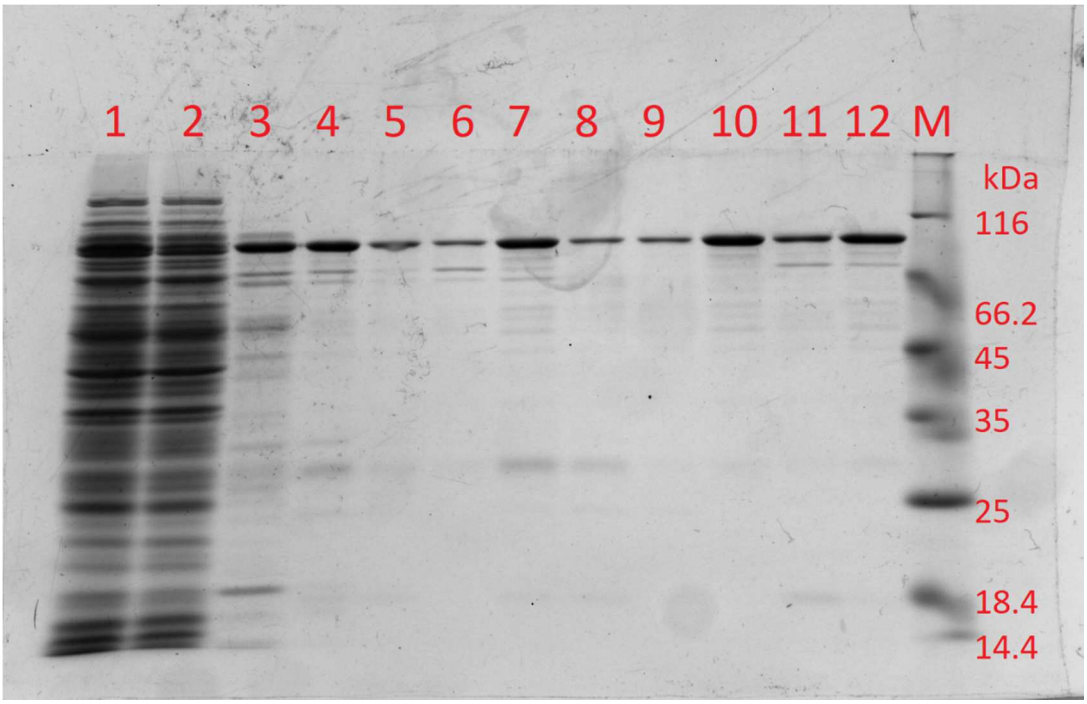

Figure 8: **SDS-PAGE of VHL purification**. Lane 1: Crude extract, 2: Ni-NTA column flow-through. Lane 3: IMAC40 wash fraction #3. Lanes 4 and 5: IMAC500 elution fractions #1 and #2 respectively. Lanes 6-8: GF fractions 27, 31, and 36 respectively. Lane 9: DEAE column flow-through. Lanes 10 and 11: DEAE fractions 16 and 20 respectively. Lane 12: Pooled DEAE fractions 16-20, final purified protein. M: Thermo MW Markers cat. no. 26610.

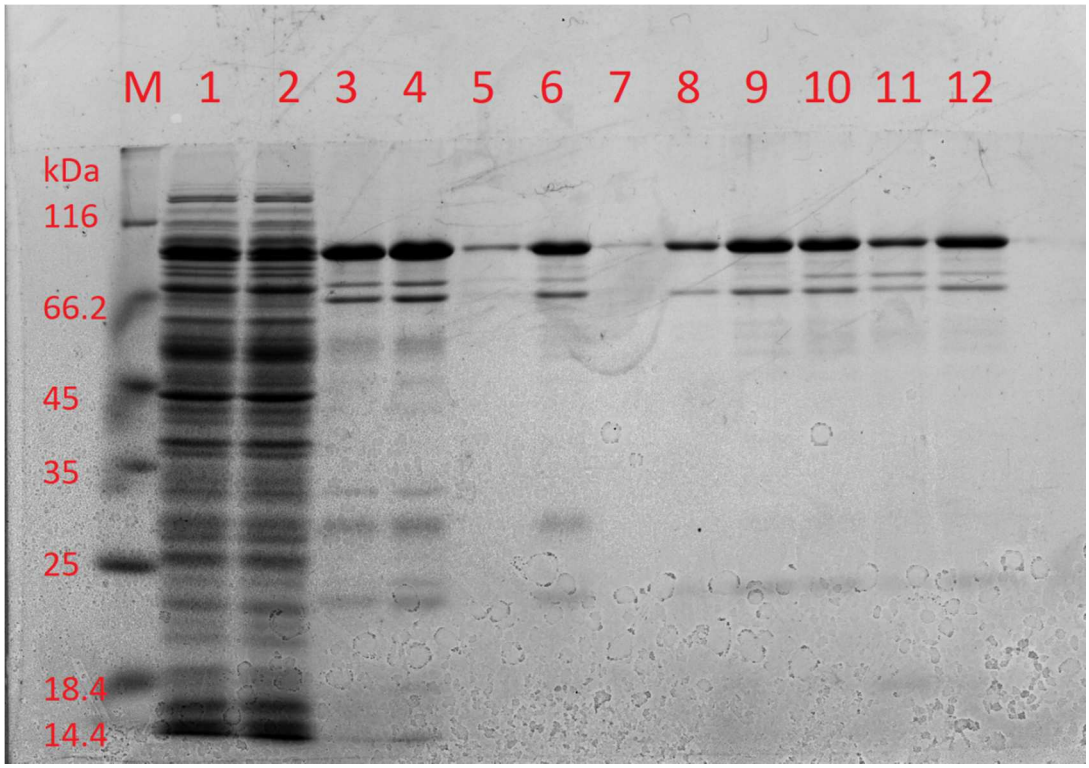

Figure 9: **SDS-PAGE of SHL purification.** M: Thermo MW Markers cat. no. 26610. Lane 1: Crude extract, 2: Ni-NTA column flow-through. Lanes 3-5: IMAC500 elution fractions #1, #2, and #3 respectively. Lane 6: Pooled GF fractions 27-34. Lane 7: DEAE column flow-through. Lanes 8-11: DEAE fractions 15, 17, 19, and 21 respectively. Lane 12: Pooled DEAE fractions 15-21, final product.

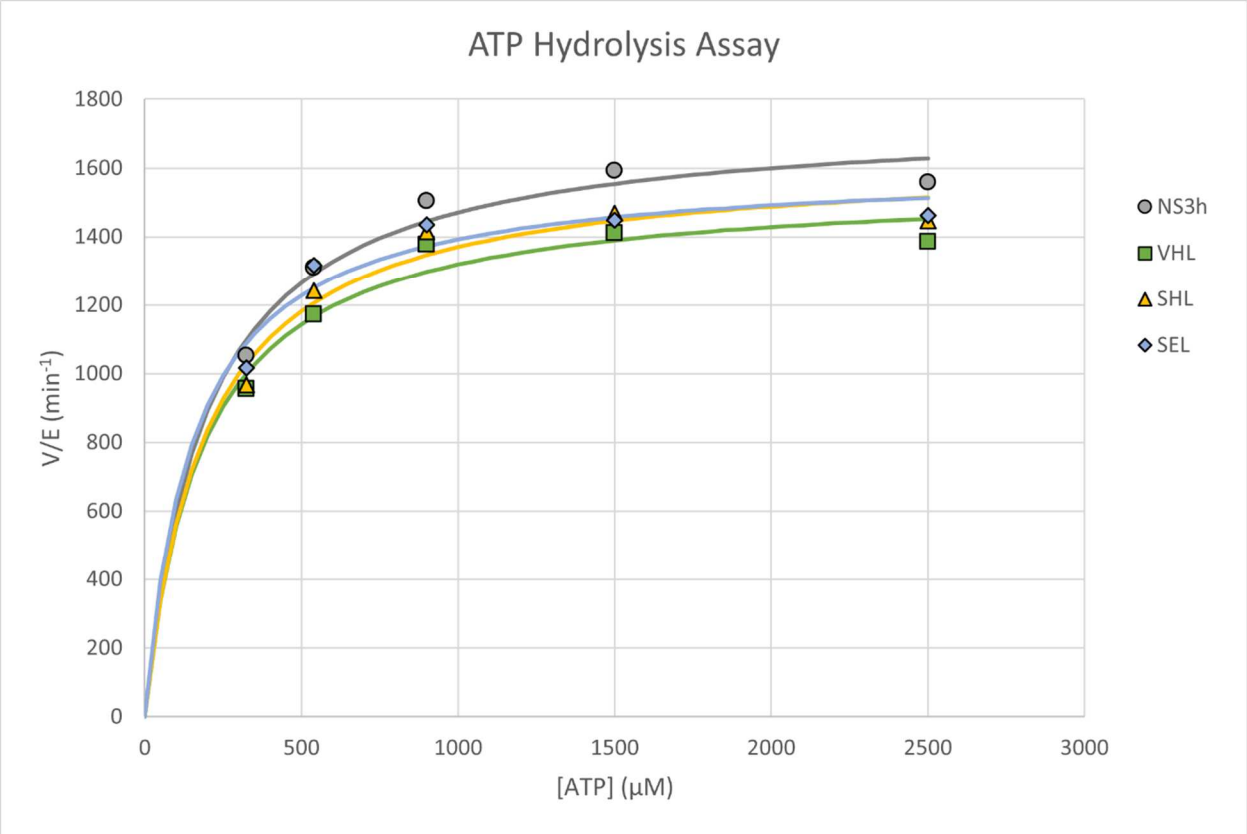

	NS3h	VHL	SHL	SEL
Vmax (µM/min)	35.1	31.1	32.6	32.1
Vmax 95% CI	30.9 to 40.0	27.0 to 36.1	28.2 to 37.9	27.7 to 37.4
k_{cat} (min^{-1})	1755	1555	1630	1605
k_{cat} 95% CI	1545 to 2000	1350 to 1805	1410 to 1895	1385 to 1870
K_M (µM)	192	181	189	154
K_M 95% CI	86.7 to 340	65.8 to 347	70.5 to 362	42.4 to 317

Figure 10: **ATP hydrolysis assay of NS3h fusion proteins compared to wild-type NS3h.** Reactions in 25 mM MOPS pH 6.5, 2 mM $MgCl_2$, 20 µM poly(U), various ATP concentrations, and 20 nM of helicase. Incubated at 23°C for 10 min and released P_i quantified by malachite green assay. Calculated Vmax, k_{cat}, and K_M values shown.

6. References

Ai, H. W., Hazelwood, K. L., Davidson, M. W., & Campbell, R. E. (2008). Fluorescent protein FRET pairs for ratiometric imaging of dual biosensors. Nature methods, 5(5), 401–403. https://doi.org/10.1038/nmeth.1207

Ben-Johny, M., Yue, D. N., & Yue, D. T. (2016). Detecting stoichiometry of macromolecular complexes in live cells using fret. Nature Communications, 7(1). https://doi.org/10.1038/ncomms13709

Biswas, S. B., Chen, P.-H., & Biswas, E. E. (1994). Structure and function of escherichia coli dnab protein: Role of the N-terminal domain in helicase activity. Biochemistry, 33(37), 11307–11314. https://doi.org/10.1021/bi00203a028

Blinkova, A., Hervas, C., Stukenberg, P. T., Onrust, R., O'Donnell, M. E., & Walker, J. R. (1993). The escherichia coli DNA polymerase III holoenzyme contains both products of the dnax gene, tau and Gamma, but only tau is essential. Journal of Bacteriology, 175(18), 6018–6027. https://doi.org/10.1128/jb.175.18.6018-6027.1993

Caruthers, J. M., & McKay, D. B. (2002). Helicase structure and mechanism. Current opinion in structural biology, 12(1), 123–133. https://doi.org/10.1016/s0959-440x(02)00298-1

Dallmann, H. G., Kim, S., Pritchard, A. E., Marians, K. J., & McHenry, C. S. (2000). Characterization of the unique C terminus of theescherichia coli τ DnaX protein. Journal of Biological Chemistry, 275(20), 15512–15519. https://doi.org/10.1074/jbc.m909257199

Dohrmann, P. R., Correa, R., Frisch, R. L., Rosenberg, S. M., & McHenry, C. S. (2016). The DNA polymerase III holoenzyme contains γ and is not a trimeric polymerase. Nucleic Acids Research, 44(3), 1285–1297. https://doi.org/10.1093/nar/gkv1510

Eisen, A., & Lucchesi, J. C. (1998). Unraveling the role of helicases in transcription. BioEssays : news and reviews in molecular, cellular and developmental biology, 20(8), 634–641. https://doi.org/10.1002/(SICI)1521-1878(199808)20:8<634::AID-BIES6>3.0.CO;2-I

Frick, D. N. (2007). The hepatitis C virus NS3 protein: a model RNA helicase and potential drug target. Current issues in molecular biology, 9(1), 1–20. https://doi.org/10.21775/cimb.009.001

Glover, B. P., & McHenry, C. S. (2000). The DnaX-binding subunits δ′ and ψ are bound to γ and not τ in the DNA polymerase III holoenzyme. Journal of Biological Chemistry, 275(5), 3017–3020. https://doi.org/10.1074/jbc.275.5.3017

Hawker, J. R., & McHenry, C. S. (1987). Monoclonal antibodies specific for the tau subunit of the DNA polymerase III holoenzyme of escherichia coli. use to demonstrate that Tau is the product of the dnaZX Gene and that both it and Gamma, the dnaz gene product, are integral components of the same enzyme assembly. Journal of Biological Chemistry, 262(26), 12722–12727. https://doi.org/10.1016/s0021-9258(18)45265-9

Kremers, G. J., Goedhart, J., van Munster, E. B., & Gadella, T. W., Jr (2006). Cyan and yellow super fluorescent proteins with improved brightness, protein folding, and FRET Förster radius. Biochemistry, 45(21), 6570–6580. https://doi.org/10.1021/bi0516273

Lohman, T. M., & Bjornson, K. P. (1996). Mechanisms of helicase-catalyzed DNA unwinding. Annual review of biochemistry, 65, 169–214. https://doi.org/10.1146/annurev.bi.65.070196.001125

McHenry, C. S. (2011). DNA replicases from a bacterial perspective. Annual Review of Biochemistry, 80(1), 403–436. https://doi.org/10.1146/annurev-biochem-061208-091655

McInerney, P., Johnson, A., Katz, F., & O'Donnell, M. (2007). Characterization of a triple DNA polymerase replisome. Molecular Cell, 27(4), 527–538. https://doi.org/10.1016/j.molcel.2007.06.019

Pritchard, A. E. (2000). A novel assembly mechanism for the DNA polymerase III holoenzyme DnaX complex: Association of Deltadelta' with DnaX4 forms DnaX3deltadelta'. The EMBO Journal, 19(23), 6536–6545. https://doi.org/10.1093/emboj/19.23.6536

Reha-Krantz, L. J., & Hurwitz, J. (1978). The dnab gene product of escherichia coli. i. purification, homogeneity, and physical properties. Journal of Biological Chemistry, 253(11), 4043–4050. https://doi.org/10.1016/s0021-9258(17)34796-8

Reyes-Lamothe, R., Sherratt, D. J., & Leake, M. C. (2010). Stoichiometry and architecture of active DNA replication machinery in Escherichia coli. Science, 328(5977), 498–501. https://doi.org/10.1126/science.1185757

Selvin, P. R. (1995). Fluorescence resonance energy transfer. Methods in Enzymology, 300–334. https://doi.org/10.1016/0076-6879(95)46015-2

Singleton, M. R., Dillingham, M. S., & Wigley, D. B. (2007). Structure and mechanism of helicases and nucleic acid translocases. Annual review of biochemistry, 76, 23–50. https://doi.org/10.1146/annurev.biochem.76.052305.11530 0